

FIG. 2. The diagram of  $\langle \omega_p^2 \rangle / \omega^2$  versus  $kT_e / m d^2 \omega^2$ .

variable for the second and the third resonance is made plausible by the fact that a smooth curve can be fitted to the experimental points in Fig. 2.

The main resonance is seen to be of different character. This resonance, however, has been explained in the theory by Herlofson, and, as a particular solution, in the theory by Gould.

Following Herlofson and taking into account the finite plasma radius and the surrounding glass walls, we can compute  $\langle \omega_p^2 \rangle / \omega^2$  for the main resonance in a homogeneous plasma column. The results of this computation are compared with the measured values of  $\langle \omega_p^2 \rangle / \omega^2$  in Table I, and the agreement is found to be good.

<sup>1</sup>D. Romell, *Nature* **167**, 243 (1951).

<sup>2</sup>A. Dattner, *Ericsson Tech.* **13**, 309, 350 (1957).

<sup>3</sup>N. Herlofson, *Arkiv Fysik* **3**, 247 (1951).

<sup>4</sup>R. W. Gould, Proceedings of the Linde Conference on Plasma Oscillations, 1959 (unpublished).

<sup>5</sup>E. Åström, *Arkiv Fysik* **19**, 163 (1961).

<sup>6</sup>P. Weissglas, *J. Nucl. Energy* **4**, 329, 336 (1962), part C.

<sup>7</sup>B. Agdur and B. Enander, *J. Appl. Phys.* **33**, 575, 581 (1962).

Table I. Measured and calculated values of  $\langle \omega_p^2 \rangle / \omega^2$  for the main resonance.

$d$ (mm)	$f$ (GHz)	1.1		1.9	
		Measured	Computed	Measured	Computed
32		2.90	2.62	2.79	2.75
20		2.79	2.80	2.99	2.98
16		3.02	2.91	3.17	3.04
12		3.06	2.95	3.16	3.07
8		2.98	3.28	3.13	3.37

### RESONANCE OSCILLATIONS IN A HOT NONUNIFORM PLASMA

Peter Weissglas

Swedish State Power Board, Vällingby, Sweden

(Received 12 February 1963)

In a previous paper,<sup>1</sup> the Boltzmann-Vlasov equation was taken as a starting point for a study of longitudinal plasma oscillations. The electron density in the steady state was assumed to be uniform and the plasma enclosed between two perfectly reflecting, infinite plane walls. A series of resonances was found for frequencies higher than the plasma frequency  $\omega_p$ . Of these resonances, only odd-order ones could be excited by

external fields. It was shown that the hydrodynamic equations give correct results when the applied frequency is close to  $\omega_p$ . For higher frequencies, details in the velocity distribution become important which cannot be described by a pressure term. Gould,<sup>2</sup> using the hydrodynamic equations, has found that in the cylindrical case one obtains a resonance of a somewhat different kind at a frequency  $\omega_p / \sqrt{2}$  in addition to what ap-

pears in the plane case.

Dattner<sup>3</sup> has recently combined his previous measurements with a determination of the electron density. Surprisingly, he found several resonances for  $\langle \omega_p^2 \rangle > \omega^2$ , where  $\langle \omega_p^2 \rangle$  is the measured mean square plasma frequency and  $\omega$  the applied frequency. The present note attempts to throw some light on these and other discrepancies between theory and experiment by considering the effects of a nonuniform electron density in the steady state.

According to Weissglas,<sup>1</sup> the resonances can be associated with standing longitudinal waves in the plasma. If the plasma has a high-density core, these waves will be damped out in about one Debye length as soon as the local plasma frequency exceeds the applied frequency. Therefore the oscillations will effectively take place in two regions near the walls. Each of these regions is much thinner than the total plasma thickness and has an average density substantially lower than the volume average for the whole plasma. As a result we would expect the resonances to appear at a higher density for a given applied frequency and to be more widely spaced than would be the case if the density were uniform. The latter effect arises because the spacing is essentially determined by how large a fraction of the oscillating region an average electron travels in one period.<sup>1</sup>

We will now use the hydrodynamic equations and a simple model for the density variation to examine the case analytically. Linearizing from the outset, we have

$$\partial \rho / \partial t + \text{div}(\rho \vec{v}) = 0, \tag{1}$$

$$\rho_0 \frac{\partial \vec{v}}{\partial t} = -\frac{e \rho_0}{m} \vec{E} - \frac{e \rho}{m} \vec{E}_0 - W^2 \text{grad} \rho, \tag{2}$$

$$\text{div} \vec{E} = -e \rho / \epsilon_0, \tag{3}$$

and, in addition, for the steady state,

$$\vec{E}_0 = -(W^2 m / e) \text{grad} \rho_0 / \rho_0. \tag{4}$$

The periodic solutions to Eqs. (1)-(4) in plane geometry ( $-L \leq x \leq L$ ) satisfy

$$\frac{d^2(\rho_0 v_x)}{dx^2} - \frac{1}{\rho_0} \frac{d\rho_0}{dx} \frac{d(\rho_0 v_x)}{dx} + \frac{\omega^2 - \omega_p^2(x)}{W^2} \rho_0 v_x = -\frac{i \omega e \rho_0}{m W^2} E(L). \tag{5}$$

Natural modes of oscillation are given by the non-trivial solutions in the absence of an applied ex-

ternal field, i. e., by the nonzero solutions of the homogeneous part of Eq. 5. We now choose

$$\rho_0(x) = \bar{\rho}_0(1 + \epsilon + \cos 2x), \quad \omega_p^2(x) = \omega_{p0}^2(1 + \epsilon + \cos 2x), \tag{6}$$

where the small number  $\epsilon$  has been included to avoid difficulties from an infinite static electric field at the boundary. Normalizing all lengths to make the walls fall at  $x = \pm \frac{1}{2}\pi$ , Eq. (5) can be written

$$\frac{1}{4} \frac{d^2 y}{dx^2} + (\alpha - 4q \cos 2x)y + \left[ \frac{-4\bar{\rho}_0(1 + \epsilon)}{\rho_0(x)} + \frac{3\bar{\rho}_0^2 \epsilon (1 + 2\epsilon)}{\rho_0^2(x)} \right] y = 0, \tag{7}$$

where the source term is excluded, and

$$\alpha = \frac{L^2(\omega^2 - \omega_{p0}^2)}{\pi^2 W^2} + 1, \quad q = \frac{L^2 \omega_{p0}^2}{4\pi^2 W^2}, \quad y = v_x \rho_0^{1/2}. \tag{8}$$

For large  $q$  values (in Dattner's experiments we have roughly  $10 < q < 1000$ ), a first approximation to the eigenvalues of (7) is obtained by neglecting the last term. We then have a Mathieu equation,<sup>4</sup> and the solutions compatible with the condition of perfectly reflecting walls are  $ce_{2n+1}$  and  $se_{2n}$ . Of these only the first kind can be excited by external fields. We now distinguish two cases,  $\epsilon \ll 1/\sqrt{q}$  and  $\epsilon \gg 1/\sqrt{q}$ . In the first case the resonance condition is determined by the details in the outer boundary layers, and by first-order perturbation theory we get the estimate

$$\frac{\omega_n^2}{\omega_{p0}^2} = \frac{1}{2q} \int_{-1/2\pi}^{1/2\pi} \frac{ce_{2n+1}(x, q)^2}{\cos^2 x} dx + O(q^{-1/2}) = \text{const} q^{-1/4} + O(q^{-1/2}), \quad n = 0, 1, 2, \dots \tag{9}$$

In the second case we can completely neglect the last term in Eq. (7), which physically originates from the influence of the static field to get

$$\frac{\omega_n^2}{\omega_{p0}^2} = [(4n + 3)/\sqrt{2}] q^{-1/2} + O(q^{-3/4}), \tag{10}$$

where the asymptotic expression for the eigenvalues of the Mathieu equation has been used.<sup>4</sup> With a uniform density, the resonance condition is in our notation

$$\frac{\omega_n^2}{\omega_{p0}^2} = 1 + \frac{1}{16}(2n + 1)^2 q^{-1}. \tag{11}$$

Comparing Eqs. (9), (10), and (11), we see that

both (9) and (10) allow several resonances below  $\omega_p$ . For large  $q$  values the spacing of the resonances according to Eqs. (9) and (10) is much larger than given by (11), as is also the case with the experimental results. It is therefore felt that the phenomenon of resonance oscillations can be fairly well explained on the basis of the present theory, although much needs to be done on calculations using a realistic density variation and an appropriate geometry before numerical comparison with experiment is possible. The unrealistic density variation we have chosen gives a too low

value for the density in the oscillating region. This fact may explain why Eq. (10) gives unreasonably large values for  $\omega_p/\omega$  at resonance.

<sup>1</sup>P. Weissglas, J. Nucl. Energy 4, 5 (1962), part C.

<sup>2</sup>R. W. Gould, Proceedings of the Linde Conference on Plasma Oscillations, 1959 (unpublished).

<sup>3</sup>Adam Dattner, preceding Letter [Phys. Rev. Letters 10, 205 (1963)].

<sup>4</sup>E. Jahnke, F. Emde, and F. Lösch, Tables of Higher Functions (McGraw-Hill Book Company, Inc., New York, 1960).

### NONELASTIC TRANSITIONS IN CHROMIUM

M. E. de Morton\*

Metallurgy Department, Manchester University, Manchester, England

(Received 7 December 1962)

Neutron diffraction measurements<sup>1</sup> have established that the second-order transition in Cr observed on cooling below 40°C occurs through the onset of antiferromagnetic ordering with magnetic moments parallel to antiphase-domain boundaries. A further change in the reflected neutron intensity found in Cr single crystals at lower temperatures, i.e., -120°C<sup>1,2</sup> and -160°C,<sup>3</sup> and termed the spin-flip transition  $T_{S-F}$ , occurs when the direction of magnetic moments spontaneously rotates through 90°.

The transition at ~40°C, the Néel temperature  $T_N$ , is accompanied by a sharp peak ( $\delta = 3 \times 10^{-3}$ ) in internal friction and a precipitous trough in the dynamic Young's modulus  $E$  when measured at resonant frequencies.<sup>4,5</sup> A small trough in  $E$  is also observed at -150°C. On the other hand, low-frequency (1 cps) internal friction measurements<sup>6</sup> on polycrystalline Cr to -70°C show contrasting results in that below  $T_N$  a marked, continuous increase in logarithmic decrement  $\delta$  occurs; moreover, damping in this region is strongly amplitude dependent. Dislocation damping was absent in these measurements due to strong impurity atom interaction.

Recent internal friction measurements continued down to -196°C are shown in Fig. 1 and indicate the magnetomechanical damping referred to above disappears below about -150°C, the spin-flip transition temperature. Vibration frequency measurements  $f$  made concurrently with  $\delta$  and shown in Fig. 2 indicate that the dynamic shear modulus  $G$ , which is proportional

to  $f^2$ , goes through a peak at  $T_N$  and below  $T_{S-F}$  increases very rapidly. These measurements, which show hysteresis, were made on annealed polycrystalline Cr of 99.98% purity and grain size of ~130  $\mu$  in a torsional pendulum at 0.1-mm pressure of helium. The magnitude of the magnetomechanical damping was found to increase with increasing grain size.

The nonelastic behavior of Cr below  $T_N$  has been interpreted on the basis of an antiferromag-

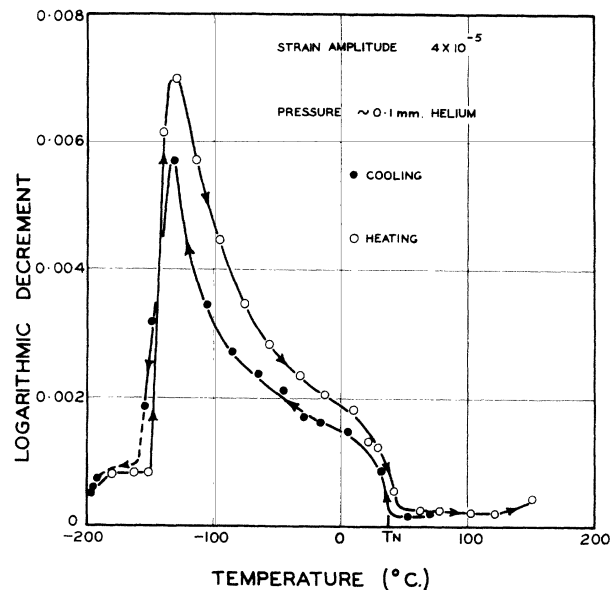


FIG. 1. Damping of chromium as a function of temperature (frequency—1 cps).